SPALLATION NEUTRON SOURCE RING – DESIGN AND CONSTRUCTION SUMMARY*

Jie Wei†

for the Spallation Neutron Source Collaboration, USA

Abstract

After six years, the delivery of components for the Spallation Neutron Source (SNS) accumulator ring (AR) and the transport lines was completed in Spring 2005. Designed to deliver 1.5 MW beam power (1.5×10^{14} protons of 1 GeV kinetic energy at a repetition rate of 60 Hz), stringent measures were implemented in the fabrication, test, and assembly to ensure the quality of the accelerator systems. This paper summarizes the design, R&D, and construction of the ring and transport systems.

INTRODUCTION

The SNS ring and transport lines designed and constructed mainly by the Brookhaven National Laboratory, will accumulate and transport pulses of 1.5×10^{14} protons of 1 GeV energy at a repetition rate of 60 Hz (Table 1) [1, 2]. The cost is about US$10.4M in R&D, US$9.2M in accelerator controls, and US$113.7M in construction

Table 1: Major parameters of the ring, High Energy Beam Transport (HEBT), and Ring to Target Transport (RTBT).

Quantity	Value
Ring circumference	248.0 m
HEBT, RTBT length (line+dump)	169+61, 151+29 m
Beam kinetic energy	1 GeV
Magnetic rigidity, $B\rho$	5.657 Tm
Average beam power	1.5 MW
Repetition rate	60 Hz
Number of protons per pulse	1.5×10^{14}
Revolution frequency	1.058 MHz
Peak RF voltage ($h = 1, 2$)	(40, 20) kV
Unnorm. emittance ($\epsilon_x + \epsilon_y$, 99%)	240 $\pi\mu$m
Betatron acceptance	480 $\pi\mu$m
RF momentum acceptance	± 1 %
Transverse tunes (ν_x, ν_y)	6.23, 6.20
Transition energy, γ_T	5.23
Natural chromaticities (ξ_x, ξ_y)	$-7.9, -6.9$
No. of super-periods	4
No. of dipole (ring, HEBT, RTBT)	39, 9, 1
Ring dipole field	0.7406 T
Ring dipole gap height	170 mm
No. of quad (ring, HEBT, RTBT)	53, 40, 32
Ring quad inner diameter	210-300 mm
No. of sext. (ring, HEBT, RTBT)	20, 0, 0
Vacuum pressure, ring	$< 10^{-8}$ Torr

including the accelerator physics role and the major subsystem delivery of magnets, power supplies, collimators, vacuum system, radio-frequency (RF) equipment, and instrumentation (Fig. 1). The total effort involved about 500 BNL full-time-equivalent-year personnel responsible for the manufacture of 331 magnets, 504 vacuum chambers, 22 collimators and scrapers, 283 power supplies, 4 RF cavities, and 441 diagnostics devices. Tunnel and infrastructure construction, target interface, installation, and commissioning are ORNL's responsibility not discussed in this paper [3].
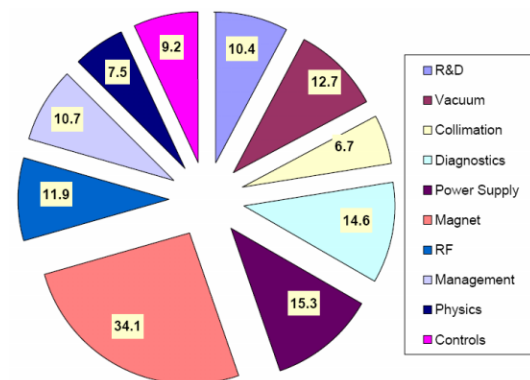

Figure 1: SNS ring design and component construction cost (in US$M) by subsystems.

R&D PROGRAMS

The R&D program mainly consisted of the conceptual design, the optimization of the lattices, and the study of beam collimation, stripping foil, and electron-cloud effects.

Beam Collimation

Beam collimation of above 90% efficiency is key to reducing uncontrolled beam-loss for hands-on maintenance of the accelerator. Demonstration of the two-stage collimation was performed at high energy at the CERN SPS. The SNS collimation studies were performed at 1.3 GeV kinetic energy at the IHEP U70 ring, Protvino, evaluating collimation efficiency in the presence of thin scrapers of carbon, silicon, and tungsten material, as well as bent crystals [4].

Several innovative ideas were adopted in the SNS collimation system. Double-walled Inconel 718 filled with a pressurized helium gas was used for the collimator beam tube to resist radiation damage and thermo-mechanical shock, and to facilitate leak detection [5, 6]. Tantalum was chosen for the thin scrapers for its large Coulomb scattering angle and durability under radiation. Layers of particle bed of stainless-steel spheres were used to absorb the transient heat load from the beam pulse [7].

Stripping Foil

The goal is single-edge supported foils of density $\sim300\mu g/cm^2$ lasting for at least days of operation under a 1.5 MW H^- beam. Foil lifetime tests were performed at BNL Linac with the 750 keV H^- beam simulating the condition of comparable foil temperature peaking above 3000 K. Chemical-vapor-deposited diamond foils demonstrated superior quality [8]. A quick-exchange mechanism was developed accommodating up to 24 foils allowing weeks of uninterrupted operations. Radiation-resistant video cameras and lenses are used to monitor the performance.

Electron-Cloud Effects

Because of the high beam intensity in an accumulator ring, beam-induced electron cloud is likely to be an intensity-limiting effect. Experiments were performed at the BNL Tandem to evaluate the grazing-angle dependence of electron secondary-emission yield (SEY) upon the incident proton beam on regular and saw-tooth surfaces [9]. Surface TiN coating parameters were determined with SEY measurement of the coated samples at CERN [10, 11]. Extensive computer simulations were performed to benchmark the observations at the LANL PSR [12].

DESIGN ITERATIONS

Design iterations occurred mostly in the early stages of construction. While challenging the project coordination, such iterations maximized the accelerator potential and optimized the deliverables within budgetary boundaries.

RCS versus AR

A study was performed comparing the AR to a rapid-cycling-synchrotron (RCS) design: a 60 Hz, 400 MeV linac feeds two, vertically stacked RCSs accelerating the proton beam to 2 GeV energy. The biggest challenge to the RCS design was from the stringent (1 W/m) beam-loss criterion: although relaxed by a factor of 5, still only 0.4% uncontrolled loss was allowed for a 2 MW beam power assuming 90% collimation efficiency. Unlike AR, the RCSs operating at 30 Hz required a high RF voltage for acceleration, a large aperture to accommodate the space charge at a lower energy, ceramic vacuum pipes with detailed RF shielding, and high-performance power supplies. Minimization of magnetic errors due to eddy current, ramping, saturation, and power-supply tracking was non-trivial. The study concluded that the required RCS design was technically more demanding and less cost effective [13].

Ring Layout

A ring lattice of four-fold symmetry was chosen over the three-fold, so that four dispersion-free straight sections could each house injection, collimation, extraction, and RF [2]. The original α transport-line layout was replaced by an Ω layout. Both decisions facilitate hands-on maintenance.

Ring FODO-Doublet Lattice

The ring straight lattice was changed from FODO to doublet to provide long uninterrupted drift space for injection, collimation, and extraction, and to improve injection and collimation efficiency [1]. The ring FODO arc, matched to the straight, allows for easy optical corrections.

1.3 GeV Linac Compatibility

Compatible with the potential of upgrading the superconducting RF linac energy from 1.0 to 1.3 GeV for a higher beam power, the ring circumference was increased from 220 m to 248 m. The 12.5 m-long uninterrupted straight reserved space for future, longer magnets for low-loss injection, and space for additional extraction kickers. All power supplies were specified for 1.3-GeV operation with a 10% margin. Magnetic interference between nearby magnets was closely monitored and compensated.

Injection System Optimization

With the doublet straight lattice, the injection system was re-designed with a symmetric layout. The lattice quads were removed from the ring H^-/H^0 injection channel, so that the lattice tuning was largely decoupled from the injection tuning [1]. Compensated, tapered magnets guide the stripped electrons to the collector [14].

Extraction System Optimization

With kicker magnets located inside the vacuum chamber, the high permeability material of the extraction system is the leading source of external beam-coupling impedance. Several iterations were made to the kicker magnets and the PFN circuit: enlarging the kicker width, terminating the PFN with a 25Ω resistance, and shielding the termination. Saturable inductors are used to isolate the PFN, shorten the rise time, and improve the pulse flatness [15, 16].

Chromatic Sextupole

Chromatic sextupoles were incorporated at a later stage of construction. Four-family sextupoles are arranged in 4-fold ring lattice symmetry to provide chromatic tuning and damping adjustments over the full momentum range without compromising the dynamic aperture [17, 18].

HEBT Energy Corrector/Spreader

The HEBT energy corrector and spreader are designed to reduce longitudinal beam halo and to facilitate longitudinal painting. Implementation is expected before the accelerator reaches the full-power capacity.

CONSTRUCTION ISSUES

During the construction, technical issues were constantly identified and resolved, demanding fast and close interaction between the physicists, engineers, and the vendors.

Magnet field Quality Iterations

Magnet measurements played a key role in both finalizing the design and qualifying each production magnet. Iterations were made on every kind of magnet for expectation of magnetic accuracy at 10^{-4} for main dipoles and quads, 10^{-3} for sextupoles, chicane, and transport magnets, and 10^{-2} for correctors at $480\pi\mu$m acceptance [19, 20]. Exceptions include a large (0.19×10^{-2}) systematic 20th pole on narrow-width quads in the straights whose effects are

negligible during the 1 ms accumulation, and large (6%) decapole in multi-coil skew-sextupole correctors [21].

Magnet Transfer Function Iterations

Excessive variations (up to 0.25%) in the magnet transfer function were measured among both dipoles and quads of solid-steel cores [20]. The dipoles were shimmed with iron sheets to achieve $<10^{-4}$ variation for 1 GeV operation, and sorted according to 1.3 GeV measurement data to minimize orbit corrector strength. The ring quads were partly sorted according to the power-supply family, and partly shimmed to achieve below 10^{-4} variation among each family. Excessive ($\sim$137 Gm) residual field measured near the ends of the circulating beam pipe of the Lambertson extraction magnet was reduced by shielding with iron pieces [21].

Injection Trial Assembly

The injection section contains the incoming line from the HEBT, the outgoing line to the injection dump, and the ring straight section with chicane, septum, and bump magnets, stripping foil and electron collection assemblies, and diagnostics. The section was trial assembled at BNL identifying many mechanical interferences. Edges of the narrow-width quads had to be trimmed and repatched to ensure proper magnetic transfer function at all design currents [21].

Diagnostics Replanning

Implemented ring and transport diagnostics include full systems of beam position, loss, current, and foil video monitors, as well as beamline components of beam-in-gap and ionization profile monitors, coherent/incoherent tune measurements, and electron detectors. A replanning was necessary to ensure the completion of the essential systems with limited funds. Such systems were successfully tested during the SNS linac commissioning [22].

Global Coordinates Confirmation

Global coordinates used for component installation were first generated from the design optics and mechanical drawings and then confirmed with the actual component survey. This process identified many mismatches. In one case, the edge (instead of the center) of the quad was mistakenly used as a reference; the difference between the mechanical and effective length of the magnet led to a 5 cm shift of the manufactured extraction kicker assembly. Fortunately, the engineering margin in the kicker power supplies allowed easy adjustments of the optics with no loss of acceptance.

Infrastructure Matching

Infrastructure parameters include power supply ratings, cooling water capacity and pressure, tunnel 3D geometry, overhead crane capacity and height, and operating temperature [23]. Parameter matching has been challenged by the need to minimize the engineering margin for budgetary savings, the design changes (e.g. addition of sextupoles; increase in tunnel temperature, magnet resistance, and power supplies), and the growing demands.

Engineering Issues

Other resolved engineering issues include copper-to-stainless steel brazing, radiation-hardened magnet coil leak identification and repair, prevention of shipping damage resulting from long transport journey to ORNL, and safety precautions during the measurement of the radiation-hardened magnets to avoid overheating.

LESSONS LEARNED

Among the overall positive experience of a multi-laboratory collaboration are some debatable lessons.

Direct and active communications at every working level between BNL and ORNL, and between BNL and every major vendors, are crucial to the project coordination. An early start of weekly conferences, frequent visits, and motivated responsibility assignment can enhance understanding and avoid work replanning.

Even though the use of solid-steel, as opposed to laminated steel, magnet cores led to later complications of magnet measurement and shimming, overall a cost saving was realized. The ring design did not allow in-situ baking of vacuum chambers that would be needed for alternative nonevaporable-getter (NEG) film coating [11].

More extensive 3D magnet modeling with actual geometry and material may reduce later measurement iterations.

SUMMARY

Quality has been BNL's first priority through the entire project. After six years and with the help from the collaboration, BNL has completed the project scope on time and within budget with minimal contingency draw. The strategic plan also allows for a straightforward upgrade towards higher beam energy and power.

We are indebted to the SNS teams and our collaborators for their devotion and contributions.

REFERENCES

[1] J. Wei et al, PRST-AB, **3** (1999) 080101; J. Wei, Rev. Mod. Phys. **75** (2003) 1383
[2] W.T. Weng, J. Alessi, et al, PAC'97 (1997) 970
[3] N. Holtkamp, PAC'03 (2003) 11
[4] N. Catalan-Lasheras et al PRST-AB **4** (2001) 010101; PAC'01 (2001) 424
[5] H. Ludewig, N. Simos, J. Walker, et al, PAC'99 (1999) 548
[6] W. Sommer et al, Materials Characterization, **43** (1999) 97
[7] N. Simos, H. Ludewig, et al, HALO'03 (2003) 167
[8] R. Shaw, R. Cutler, A.D. Herr, et al, PAC'03 (2003) 617
[9] P. Thieberger et al, Phys. Rev. A, **61** (1999) 042901
[10] R. Todd, H. Hseuh, P. He, D. Weiss, these proceedings
[11] H. Hseuh, M. Blaskiewicz, P. He, et al, these proceedings
[12] L. Wang et al, these proceedings
[13] J. Wei et al, EPAC00 (2000) 981
[14] Y.Y. Lee, G. Mahler, W. Meng, et al, these proceedings
[15] D. Davino, H. Hahn, Y.Y. Lee, EPAC'02 (2002) 1467
[16] W. Zhang, H. Hahn, J.-L. Mi, et al EPAC'04 (2004) 1810
[17] N. Tsoupas, C. Gardner, et al, EPAC'00 (2000) 1581
[18] Y. Papaphilippou, D.T. Abell, EPAC'00 (2000) 1453
[19] J. Tuozzolo, J. Alduino, et al, PAC'03 (2003) 2156
[20] P. Wanderer, J. Jackson, A. Jain et al, EPAC'02 1317
[21] D. Raparia, these proceedings
[22] C. Dawson et al, Beam Instrum. Workshop (2002) 376
[23] W. McGahern, V. Badea, M. Hemmer et al, EPAC'04 1565